

**Exciton Peierls mechanism and universal many-body gaps in carbon nanotubes**Maria Hellgren,<sup>1</sup> Jacopo Baima,<sup>2</sup> and Anissa Acheche<sup>1</sup><sup>1</sup>*Sorbonne Université, Muséum National d'Histoire Naturelle, UMR CNRS 7590, IRD, Institut de Minéralogie, de Physique des Matériaux et de Cosmochimie, IMPMC, 4 place Jussieu, 75005 Paris, France*<sup>2</sup>*Sorbonne Université, UMR CNRS 7588, Institut des Nanosciences de Paris, INSP, 4 place Jussieu, 75005 Paris, France*

(Received 28 February 2018; revised manuscript received 12 July 2018; published 8 November 2018)

“Metallic” carbon nanotubes exhibit quasiparticle gaps when isolated from a screening environment. The gap-opening mechanism is expected to be of electronic origin, but the precise nature is debated. In this work, we show that hybrid density functional theory predicts a set of excitonic instabilities capable of opening gaps of the size found in experiment. The excitonic instabilities are coupled to vibrational modes and, in particular, the modes associated with the  $\Gamma - E_{2g}$  and  $\mathbf{K} - A'_1$  Kohn anomalies of graphene, inducing Peierls lattice distortions with a strong electron-phonon coupling. In the larger tubes, the longitudinal optical phonon mode becomes a purely electronic dimerization that is fully symmetry conserving in the zigzag and chiral tubes, but breaks the symmetry in the armchair tubes. The resulting gaps are universal (i.e., independent of chirality) and scale as  $1/R$  with tube radius.

DOI: [10.1103/PhysRevB.98.201103](https://doi.org/10.1103/PhysRevB.98.201103)

Low-dimensional carbon systems have been the subject of intense research for the last two decades, both for their promise as building blocks in future nanoelectronic devices and for their novel fundamental physical properties [1]. In reduced dimensions, the electron-electron (e-e) interaction is expected to play an increasing role, driving phenomena such as edge magnetism [2], exciton condensation [3], and superconductivity [4,5]. Important examples are the quasi-one-dimensional carbon nanotubes (CNTs) that exhibit a wide range of features depending on their radius and chirality [6]. Within a single-particle description, some CNTs are predicted to be semiconducting while others metallic. However, in a pioneering experiment [7], it was demonstrated that the e-e interaction induces gaps in all “metallic” CNTs—if suspended in a clean environment. This observation was recently confirmed to be universal, i.e., independent of chirality [8].

The physical origin of the observed quasiparticle gaps has not yet been settled. First-principles calculations have mainly focused on Peierls transitions, driven by the electron-phonon interaction [9–13]. Local functionals in density functional theory (DFT) predict soft phonon modes and lattice instabilities associated with the  $\mathbf{K} - A'_1$  Kohn anomaly of graphene [14]. The Peierls gaps are, however, an order of magnitude too small and scale as  $1/R^3$  with tube radius, in contrast to the approximate  $1/R$  behavior found in experiment. On the other hand, in Ref. [15], calculations were performed with an improved description of the e-e interaction via hybrid DFT, showing that the picture can change. If the long-range Coulomb interaction is accounted for, small armchair CNTs exhibit Peierls distortions already in the unit cell. Although this study points toward larger gaps, they again appear to decay quickly with tube radius.

Purely electronic mechanisms such as excitonic instabilities, or electronic charge density waves, also driven by the long-range Coulomb interaction, have been shown to produce the correct scaling with tube radius [16–21]. Such an

instability was recently studied with *ab initio* quantum Monte Carlo (QMC) in the (3,3) armchair tube, and a stable charge-transfer electronic state that breaks the sublattice symmetry was found [21]. Calculated gaps were, however, more than an order of magnitude smaller than experimental observations. In addition, most theoretical studies have focused on the armchair family of CNTs. It is, therefore, not clear which theories can account for the weak chirality dependence.

In this work, we present a mechanism based on a unified picture of Peierls distortions and excitonic instabilities. We employ first-principles hybrid DFT that captures the long-range exchange interaction, crucial to describe both excitonic and lattice instabilities in suspended CNTs. We then show that the  $A_1$  longitudinal optical phonon mode is unstable, leading to a Peierls distortion, or dimerization, which is fully symmetry conserving in the zigzag and chiral tubes, but breaks the mirror symmetry in the armchair tubes. The lattice distortion is shown to be coupled to a purely electronic instability of the same symmetry, allowing the dimerization to be formed spontaneously already at the electronic level. For the larger tubes, the lattice distortion vanishes while the electronic instability remains and becomes degenerate within a multiplet of excitonic states. The corresponding gaps are universal and in good quantitative agreement with experiments.

To the nominally metallic CNTs belong the  $(n, n)$  armchair ( $\mathcal{A}$ ) tubes, the  $(3n, 0)$  zigzag ( $\mathcal{Z}$ ) tubes, and the  $(3l + n, n)$  chiral ( $\mathcal{C}$ ) tubes ( $n$  and  $l$  being integers). By applying periodic boundary conditions to the band structure of a rolled graphene sheet (zone-folding approximation), these tubes inherit the two Dirac points formed by the  $\pi$  and  $\pi^*$  bands of graphene. The position of the Dirac points depends on the chirality, ranging from  $K = \pm 1/3$  in  $\mathcal{A}$  tubes to the two degenerate Dirac points at  $\Gamma$  in the  $\mathcal{Z}$  tubes. In the case of  $\mathcal{A}$  tubes, the Dirac point is protected against symmetry-preserving perturbations, while in the  $\mathcal{Z}$  and  $\mathcal{C}$  tubes, different mechanisms such as curvature or strain can open a small gap at the Fermi level [6].

An atomic displacement along a phonon mode can also open a gap, provided the electron-phonon coupling (EPC) mixes valence and conduction states [9,13]. It is well known that in graphene, the  $\Gamma - E_{2g}$  and  $\mathbf{K} - A'_1$  phonon modes are significantly softened by the EPC, displaying a Kohn anomaly [14,22]. Within local approximations in DFT, it has been shown that the strong EPC carries over to metallic CNTs and is enhanced by confinement [13,23]. The degenerate  $\Gamma - E_{2g}$  mode splits into a longitudinal-optical (LO) and a transverse-optical (TO) mode, where the frequency of the LO mode is softened since the distortion along this pattern opens a gap [9]. Similarly, the  $\mathbf{K} - A'_1$  mode of graphene turns into a  $2k_F$  mode in the  $\mathcal{A}$  and  $\mathcal{C}$  tubes, and a  $\Gamma$  mode (which breaks the rotational symmetry) in the  $\mathcal{Z}$  tubes. Depending on the strength of the EPC, the soft phonon frequency may result in a permanent lattice distortion with a gap, i.e., a Peierls transition. This has been shown to occur for different modes in some small CNTs. The strength of the mixing is, however, sensitive to how the e-e interaction is treated and, in particular, to the long-range part of the exchange interaction [22,24]. If strong enough, the orbitals could mix spontaneously, i.e., solely due to the e-e interaction, without the need for an atomic displacement. This would lead to an excitonic insulator state, as formulated in Refs. [25,26].

Let us denote the valence ( $\pi$ ) and conduction ( $\pi^*$ ) orbitals of the CNT by  $\varphi_{v,k}$  and  $\varphi_{c,k}$ , where the index  $k$  is the momentum relative to the valley the orbital belongs to. The mixed orbitals (that must break the symmetry in the  $\mathcal{A}$  tubes, but not necessarily in the  $\mathcal{Z}$  and  $\mathcal{C}$  tubes) can be written as linear combinations of the unperturbed orbitals,

$$\tilde{\varphi}_{v,k} = u_k \varphi_{v,k} + v_k \varphi_{c,k}, \quad (1)$$

$$\tilde{\varphi}_{c,k} = u_k^* \varphi_{c,k} - v_k^* \varphi_{v,k}. \quad (2)$$

For a purely electronic instability, the new wave function is constructed as an antisymmetrized product of the mixed valence orbitals, i.e.,

$$|\Psi\rangle = \prod_k \tilde{\varphi}_{v,k}^\dagger |0\rangle = \prod_k (u_k + v_k \varphi_{c,k}^\dagger \varphi_{v,k}) |\Phi\rangle, \quad (3)$$

where  $|0\rangle, |\Phi\rangle$  are the vacuum, and “high-symmetry” or “single-particle” ground states, respectively. The last equality is easily derived and demonstrates the excitonic nature of the new ground state. In a single-particle description, the symmetry of the Hamiltonian is always preserved. However, within a self-consistent field (SCF) method, such as Hartree-Fock (HF) or DFT, the effective self-consistent HF or Kohn-Sham potential may break the symmetry of the original Hamiltonian. In this way, a symmetry-broken excitonic state can also be described as a single Slater determinant built up from the orbitals  $\tilde{\varphi}_{v,k}$ , generated by the symmetry-broken Hamiltonian. However, in standard semilocal approximations within DFT, such as PBE (Perdew-Burke-Ernzerhof), the long-range exchange interaction, responsible for the electron-hole coupling or excitonic effects, is not well described. By mixing in a fraction  $\alpha$  of HF exchange (typically around 25%), electronic properties generally improve as compared to pure PBE and excitonic effects are captured [27,28]. In the Supplemental

Material [29], we demonstrate how an excitonic instability can be captured with a hybrid functional.

Although the essential physics is described by the  $\pi$  and  $\pi^*$  bands, in this work we carry out first-principles simulations that include all states of the CNTs. This is achieved with the CRYSTAL program [30,31], which uses atom-centered Gaussian basis functions, which allow for an efficient evaluation of the HF exchange [32,33]. Hybrid functionals have been shown to reasonably well reproduce the many-body enhancement of the EPC in graphene [22]. In Ref. [15],  $\alpha$  was optimized to 30% for CNTs, using the experimentally determined gap and Peierls distortion in *trans*-polyacetylene [a one-dimensional (1D),  $sp_2$  bonded system with similar electronic structure to CNTs]. In this work, we therefore use this fraction of exchange and denote the approximation by HYB30.

We start by analyzing the (10,10)  $\mathcal{A}$  tube ( $R = 0.68$  nm), for which the semilocal PBE and the short-range hybrid HSE06 functionals stabilize a gapless symmetric state. With the HYB30 approximation, we find this state to be unstable with respect to a distortion along the  $A_{1u}$ (LO) phonon mode [Fig. 1(a)]. This distortion opens a gap of 124 meV [orange curve in Fig. 1(e)] and breaks horizontal and vertical mirror symmetries. A similar Peierls-like distortion was found in the smaller tubes in Ref. [15], while within PBE a softened phonon mode is observed [9]. If we now fix the lattice at the symmetric configuration (i.e., the undistorted structure) but allow for the same symmetry to break in the SCF potential, we obtain an electronic broken-symmetry state or a bond density wave [19], following the same pattern as the Peierls distortion [see Fig. 1(b)]. The dimerized bonding pattern thus occurs spontaneously, prior to the lattice distortion. In the Supplemental Material [29], we demonstrate that this corresponds to a particular orbital mixing or an excitonic instability. The purely e-e interaction-induced gap accounts for as much as 80% of the gap in the (10,10) tube, as demonstrated in Fig. 1(e).

A symmetry analysis (see Supplemental Material [29] and [34]) shows that it is also possible to mix the orbitals with a different phase of  $v_k$ , breaking the sublattice symmetry. This results in a charge transfer between the atoms, as in the “dual” charge density wave state of Ref. [19], and corresponds to the solution found by QMC [21]. This state is coupled to a radial optical (RO) phonon mode of  $A_{2g}$  symmetry, as displayed in Fig. 1(c). As the  $A_{1u}$ (LO) and  $A_{2g}$ (RO) mixings differ only by the phase of  $v_k$  and descend from a doublet of nearly degenerate excitonic states (see Supplemental Material [29] and [35,36]), they are expected to be close in energy. Indeed, starting from the symmetric configuration and by selectively switching off symmetry constraints, we could also stabilize the RO state, being only slightly higher in energy. This state is, however, only weakly coupled to the lattice and thus no further stabilization occurs. This can be understood from the fact that the corresponding out-of-plane optical (ZO) mode in graphene has no EPC. The dimerized LO state is therefore found to be the ground state in all ( $n, n$ ) tubes with  $n \geq 10$ .

In the  $\mathcal{Z}$  tubes, the LO mode is a totally symmetric  $A_{1g}$  mode [9]. In Fig. 2, we present the results for the (15,0) tube, which has a similar radius ( $R = 0.58$  nm) to the (10,10) tube discussed above. In this case, the PBE and HSE06 functionals

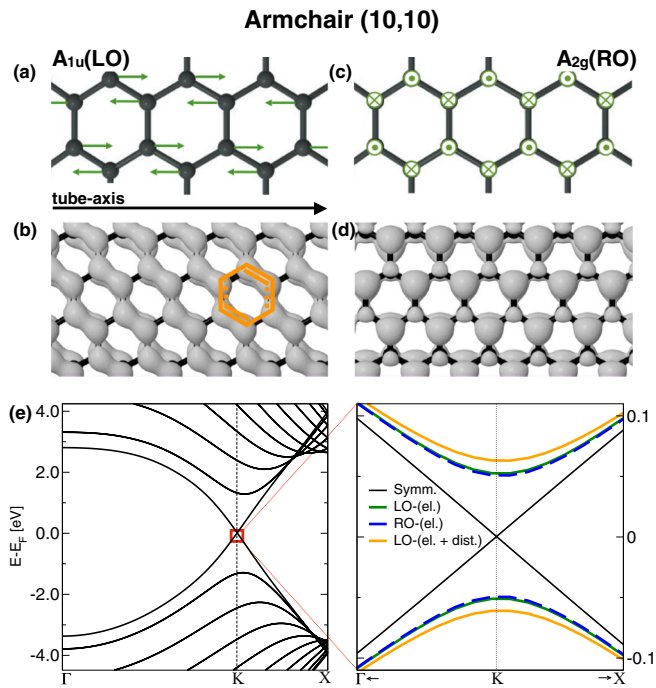


FIG. 1. (a),(c) Displacement pattern of the LO and RO modes in the  $\mathcal{A}$  tubes. (b),(d) Density obtained from states within 50 meV below the top of the valence band. (e) Left: Band structure of the high-symmetry phase of the (10,10) tube. Right: A zoom around the Fermi level. The gap of the LO mode is shown with (el. + dist.) and without (el.) lattice relaxation, and compared to that of the RO.

open small gaps of the order of a few meV. The HYB30 functional increases the gap substantially, up to 165 meV at relaxed geometry. It is often assumed that HF theory can only enhance single-particle gaps obtained at the PBE level. In the present case, such an enhancement is, however, expected to be much smaller [37]. We will now show that the HYB30 gaps are qualitatively different from the PBE gaps. If we move the atoms along the  $A_{1g}$ (LO) pattern, we find the PBE gaps to vanish, as expected from a single-particle effect. In contrast, if we use HYB30, only a minimum is reached, at around 110 meV (corresponding to 65% of the gap at relaxed geometry). To the left in Fig. 2(b), we show the dimerized charge density close to the Fermi energy. This is the  $A_{1g}$ (LO) dimerized pattern. Despite the absence of symmetry breaking, the physical mechanism is the same as in the  $\mathcal{A}$  tubes, i.e., a dimerization along the LO mode. The similarity to  $\mathcal{A}$  tubes is further emphasized by the fact that we also find a charge-transfer solution at higher energy. In order to induce this state, we have to remove the preference determined by the EPC and start from the minimum-gap geometry with the proper symmetry constraints switched off [see Fig. 2(d)].

The  $\mathcal{C}$  tubes have larger unit cells and less symmetry than the  $\mathcal{A}$  and  $\mathcal{Z}$  tubes, and exhibit only near LO and TO modes [13]. The near LO mode is a totally symmetric mode like in the  $\mathcal{Z}$  tubes. The  $\mathcal{C}$  and  $\mathcal{Z}$  tubes, thus, behave very similarly. In this work, we have called the metal-insulator transition (MIT) excitonic due to the importance of long-range interactions, but we note that the excitonic insulator state is usually assumed to

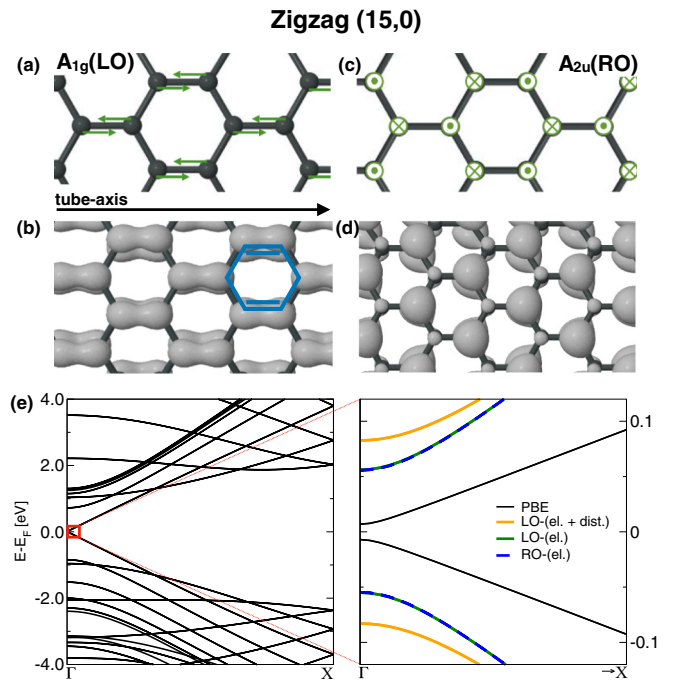


FIG. 2. (a),(c) Displacement pattern of the LO and RO modes in the  $\mathcal{Z}$  tubes. (b),(d) Density obtained from states within 50 meV below the top of the valence band. (e) Left: PBE band structure of (15,0) tube. Right: A zoom around the Fermi level. The gap of the LO mode is shown with (el. + dist.) and without (el.) lattice relaxation, and compared to that of the RO.

involve symmetry breaking [38]. Symmetry-conserving MITs of electronic origin are often called Mott transitions.

We now extend the analysis to larger CNTs ( $R > 0.7$  nm). In Fig. 3, we compare our computed gaps for the fully relaxed LO states in the  $\mathcal{A}$ ,  $\mathcal{Z}$ , and some  $\mathcal{C}$  tubes, with the low-temperature experiment performed by Deshpande *et al.* [7]. Our results match experiment rather well and, in this range of radii, the calculated gaps are close to independent of chirality. The presence of a lattice instability induces a small deviation from the excitonic  $1/R$  behavior [21] at low enough temperature. Around  $R = 1.5$  nm, the lattice contribution vanishes and the gaps become purely electronic. The electronic gaps of the  $\mathcal{A}$  tubes (dashed orange line) follow a perfect  $1/R$  behavior in the whole range, which allows us to extrapolate the results for  $R > 1.6$  nm, indicated by the full orange line. The electronic states in the larger CNTs are highly degenerate, and possibly infinitely degenerate (i.e., a complete phase invariance of the ground state). We note, however, that a strong EPC is likely to destroy supertransport properties associated with the excitonic ground state [39]. We also recall the approximate nature of the hybrid functional which tends to underestimate the lattice distortion [15]. The magnitude of the gaps varies as  $\alpha^2$ . To illustrate how a variation of  $\alpha$  affects the gaps, we have added an “error bar” in Fig. 3. Within a realistic range ( $0.2 < \alpha < 0.4$ ), the gaps are compatible with all experimental results presented so far [7,8]. We note that even on the lower bound, we have a substantial gap opening.

We now turn to the smaller CNTs for which lattice instabilities become increasingly important. The electronic states

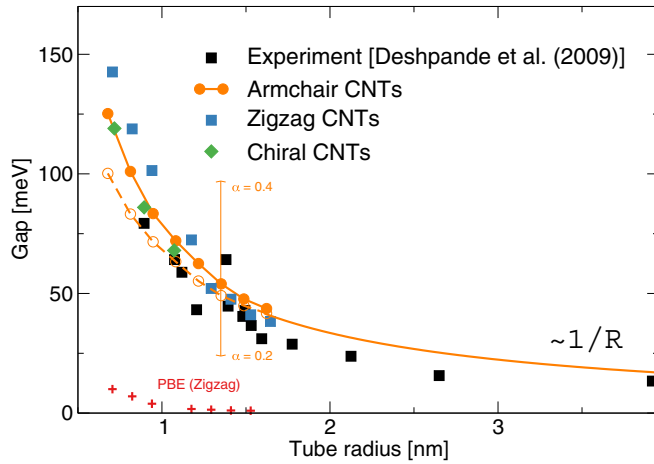


FIG. 3. Exciton-Peierls gaps in comparison with experiment (black squares). The orange circles (blue squares) correspond to the fully relaxed states of the  $\mathcal{A}$  ( $\mathcal{Z}$ ) tubes. The dashed orange line is an interpolation of the electronic gaps of the  $\mathcal{A}$  tubes, extrapolated with a  $1/R$  fit (full orange line). The green diamonds are  $\mathcal{C}$  tubes [(16,4),(20,5),(24,6)].

split in energy already by the e-e interaction, with the  $A_1$ -Peierls state always lower in energy. The splitting becomes larger as the tube is smaller similarly to what is found for excitonic states in small semiconducting CNTs [35,36,40,41]. For the small nanotubes, we also find a structural relaxation along the  $A_2(\text{RO})$  phonon mode associated with the charge-transfer electronic state. We focus on the (3,3) tube, which is interesting in its own right as CNTs of this radius have been reported to superconduct up to 15 K [4]. In addition to the  $\Gamma$  transitions, we also study the  $2k_F$  instabilities. As  $2k_F$  is incommensurate with the lattice, we can, however, only study this instability approximately. We found that for the (3,3) tube, a cell which is seven times larger than the original cell approximates  $2k_F$  within 1.1%. By relaxing the density in this supercell, we found, indeed, a symmetry-broken solution of electronic origin (see Supplemental Material [29]). At the electronic level, this state is less stable than the ones at  $\Gamma$ , as shown in Fig. 4, which again follows the trend of the splitting between exciton binding energies [36]. However, the strength of the electron-lattice interaction in such a small tube is very large and a lattice instability is present even with local functionals [11,12]. As can be seen in Fig. 4, the interaction with the lattice increases the  $2k_F$  gap by a factor of 5 and inverts the stability order, turning the  $2k_F$  instability into the

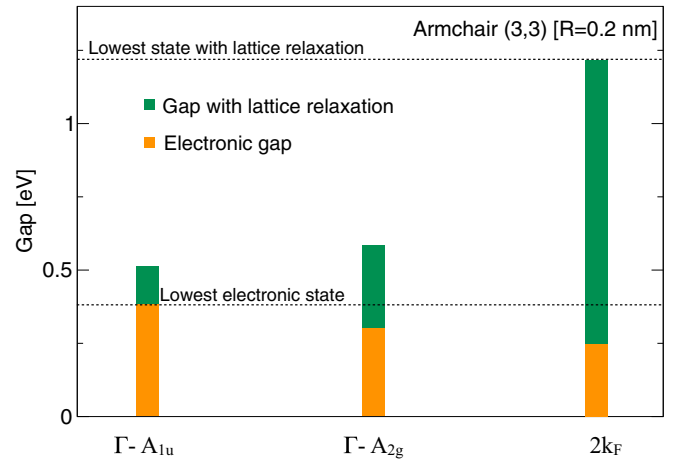


FIG. 4. Comparison between gaps from the different instabilities in the (3,3) tube. The gaps are decomposed into the electronic part (orange) and the part obtained after lattice relaxation (green). In all cases, larger gaps correspond to more stable states.

lowest state for the (3,3) tube. The role of the long-range e-e interaction is, however, still very important. In Table S1 of the Supplemental Material [29], we compare our results for the phonon frequencies to PBE data from Ref. [11]. We see that the instability with HYB30 is substantially stronger and broader in reciprocal space. With increasing radius, the  $2k_F$  lattice contribution reduces quickly, turning the  $2k_F$  instability purely electronic and degenerate with the  $\Gamma$  instabilities.

In conclusion, we have formulated a universal gap-opening mechanism in metallic CNTs based on dimerization that takes into account both electronic and lattice degrees of freedom. In the  $\mathcal{Z}$  and  $\mathcal{C}$  tubes, the gaps appear without any symmetry breaking, while in the  $\mathcal{A}$  tubes, they are induced by a Peierls lattice instability that breaks the symmetry. We have shown that these seemingly different phenomena share the same origin in an electronic transition associated with the  $A_1(\text{LO})$  phonon mode. While the electron-lattice interaction is crucial in the smaller tubes, in the experimentally observed range of diameters the electronic transition dominates and yields gaps that can reproduce experimental findings.

This work was performed using HPC resources from GENCI-TGCC/CINES/IDRIS (Grant No. DARI A0030907625).

- [1] V. Meunier, A. G. S. Filho, E. B. Barros, and M. S. Dresselhaus, *Rev. Mod. Phys.* **88**, 025005 (2016).
- [2] Y.-W. Son, M. L. Cohen, and S. G. Louie, *Nature (London)* **444**, 347 (2006).
- [3] J.-J. Su and A. H. MacDonald, *Phys. Rev. B* **95**, 045416 (2017).
- [4] Z. K. Tang, L. Zhang, N. Wang, X. X. Zhang, G. H. Wen, G. D. Li, J. N. Wang, C. T. Chan, and P. Sheng, *Science* **292**, 2462 (2001).

- [5] Y. Cao, V. Fatemi, S. Fang, K. Watanabe, T. Taniguchi, E. Kaxiras, and P. Jarillo-Herrero, *Nature (London)* **556**, 43 (2018).
- [6] J.-C. Charlier, X. Blase, and S. Roche, *Rev. Mod. Phys.* **79**, 677 (2007).
- [7] V. V. Deshpande, B. Chandra, R. Caldwell, D. S. Novikov, J. Hone, and M. Bockrath, *Science* **323**, 106 (2009).
- [8] M. J. Senger, D. R. McCulley, N. Lotfizadeh, V. V. Deshpande, and E. D. Minot, *Phys. Rev. B* **97**, 035445 (2018).



- [9] O. Dubay, G. Kresse, and H. Kuzmany, *Phys. Rev. Lett.* **88**, 235506 (2002).
- [10] X. Blase, L. X. Benedict, E. L. Shirley, and S. G. Louie, *Phys. Rev. Lett.* **72**, 1878 (1994).
- [11] K.-P. Bohnen, R. Heid, H. J. Liu, and C. T. Chan, *Phys. Rev. Lett.* **93**, 245501 (2004).
- [12] D. Connétable, G.-M. Rignanese, J.-C. Charlier, and X. Blase, *Phys. Rev. Lett.* **94**, 015503 (2005).
- [13] S. Piscanec, M. Lazzeri, J. Robertson, A. C. Ferrari, and F. Mauri, *Phys. Rev. B* **75**, 035427 (2007).
- [14] S. Piscanec, M. Lazzeri, F. Mauri, A. C. Ferrari, and J. Robertson, *Phys. Rev. Lett.* **93**, 185503 (2004).
- [15] G. Dumont, P. Boulanger, M. Côté, and M. Ernzerhof, *Phys. Rev. B* **82**, 035419 (2010).
- [16] R. Egger and A. O. Gogolin, *Phys. Rev. Lett.* **79**, 5082 (1997).
- [17] C. Kane, L. Balents, and M. P. A. Fisher, *Phys. Rev. Lett.* **79**, 5086 (1997).
- [18] H. Yoshioka and A. A. Odintsov, *Phys. Rev. Lett.* **82**, 374 (1999).
- [19] A. A. Nersesyan and A. M. Tsvelik, *Phys. Rev. B* **68**, 235419 (2003).
- [20] M. Rontani, *Phys. Rev. B* **90**, 195415 (2014).
- [21] D. Varsano, S. Sorella, D. Sangalli, M. Barborini, S. Corni, E. Molinari, and M. Rontani, *Nat. Commun.* **8**, 1461 (2017).
- [22] M. Lazzeri, C. Attaccalite, L. Wirtz, and F. Mauri, *Phys. Rev. B* **78**, 081406 (2008).
- [23] M. Lazzeri, S. Piscanec, F. Mauri, A. C. Ferrari, and J. Robertson, *Phys. Rev. B* **73**, 155426 (2006).
- [24] M. Hellgren, J. Baima, R. Bianco, M. Calandra, F. Mauri, and L. Wirtz, *Phys. Rev. Lett.* **119**, 176401 (2017).
- [25] D. Jérôme, T. M. Rice, and W. Kohn, *Phys. Rev.* **158**, 462 (1967).
- [26] A. Kozlov and L. Maksimov, *Sov. Phys. JETP* **21**, 1184 (1965).
- [27] J. Paier, M. Marsman, and G. Kresse, *Phys. Rev. B* **78**, 121201 (2008).
- [28] A. M. Ferrari, R. Orlando, and M. Rérat, *J. Chem. Theory Comput.* **11**, 3245 (2015).
- [29] See Supplemental Material at <http://link.aps.org/supplemental/10.1103/PhysRevB.98.201103> for further details on the HF excitonic ground state, symmetry of the CNT orbitals, and additional data on the  $2k_F$  instability of the (3,3) tube.
- [30] R. Dovesi, R. Orlando, A. Erba, C. M. Zicovich-Wilson, B. Civalieri, S. Casassa, L. Maschio, M. Ferrabone, M. De La Pierre, P. D'Arco, Y. Noël, M. Causà, M. Rérat, and B. Kirtman, *Int. J. Quantum Chem.* **114**, 1287 (2014).
- [31] Y. Noël, P. D'Arco, R. Demichelis, C. M. Zicovich-Wilson, and R. Dovesi, *J. Comput. Chem.* **31**, 855 (2010).
- [32] We use a modified 6-31G\* basis set [33] and fully converge the sampling of the first Brillouin zone (up to 1800  $k$  points for the  $\mathcal{A}$  tubes).
- [33] R. Demichelis, Y. Noël, P. D'Arco, M. Rérat, C. M. Zicovich-Wilson, and R. Dovesi, *J. Phys. Chem. C* **115**, 8876 (2011).
- [34] T. Vuković, I. Milošević, and M. Damnjanović, *Phys. Rev. B* **65**, 045418 (2002).
- [35] C. D. Spataru, S. Ismail-Beigi, R. B. Capaz, and S. G. Louie, *Phys. Rev. Lett.* **95**, 247402 (2005).
- [36] T. Ando, *J. Phys. Soc. Jpn.* **75**, 024707 (2006).
- [37] L. Aspitarte, D. R. McCulley, A. Bertoni, J. O. Island, M. Ostermann, M. Rontani, G. A. Steele, and E. D. Minot, *Sci. Rep.* **7**, 8828 (2017).
- [38] W. Kohn, *Phys. Rev. Lett.* **19**, 439 (1967).
- [39] B. Zenker, H. Fehske, and H. Beck, *Phys. Rev. B* **90**, 195118 (2014).
- [40] R. Matsunaga, K. Matsuda, and Y. Kanemitsu, *Phys. Rev. Lett.* **101**, 147404 (2008).
- [41] E. Chang, D. Prezzi, A. Ruini, and E. Molinari, [arXiv:cond-mat/0603085](https://arxiv.org/abs/cond-mat/0603085).